

Integrating the extracellular, intracellular, and intercellular pathogenic processes of the microbiome through glucose saturation, inhibition of the acetyl-CoA carboxylase subunit *accA* with asRNA, and through quantifying cell-to-cell quorum sensing

Tatiana Hillman ^{Corresp.} 1

¹ Department of the Biological Sciences, TheLAB, Inc., Los Angeles, California, United States

Corresponding Author: Tatiana Hillman

Email address: thillman@usc.edu

Bacteria ferment the glucose, from fiber, into Short Chain Fatty Acids, which help regulate many biochemical processes and pathways. We cultured *Escherichia coli* in Luria Broth enhanced with 15mM and 5mM of glucose. The 15mM concentration of qPCR products measured, for the target gene *accA* was 4,210 ng/μL. The 7.5μM sample had a concentration equaled to 375 ng/μL, and the 0μM sample had an *accA* concentration of 196 ng/μL. The gene *accA*, 1 of 4 subunits for the Acetyl-CoA Carboxylase enzyme, was suppressed by asRNA, producing a qPCR concentration of 63ng/μL. Antisense RNA for *accA* reduced the amount of Lux-S, a vital gene needed for propagating quorum-sensing signal molecules. Our purpose was to provide a more cumulative perspective for the pathogenesis of disease within the microbiome.

1 **Integrating the Extracellular, Intracellular,**
2 **and Intercellular Pathogenic Processes of**
3 **the Microbiome through Glucose**
4 **Saturation, Genetic Inhibition of the**
5 **Acetyl-CoA Carboxylase Subunit *accA* with**
6 **asRNA, and through the Quantification of**
7 **Bacterial Cell-to-Cell Quorum Sensing**

8 **Tatianna Hillman¹**

9 ¹603 E. University Drive, Suite B, 613, Carson CA 90746

10 ²TheLAB Inc., 1927 Zonal Avenue Los Angeles, CA 90033

11 Corresponding author:

12 Tatianna Hillman¹

13 Email address: thillman@usc.edu

14 **ABSTRACT**

Bacteria ferment the glucose, from fiber, into Short Chain Fatty Acids, which help regulate many biochemical processes and pathways. We cultured *Escherichia coli* in Luria Broth with 15mM and 5mM concentrations of glucose. The 15mM concentration qPCR measured, for, *accA* was 4,210 ng/u L. The 7.5u M sample's concentration equaled 375 ng/u L, and the 0u M sample had an *accA* concentration of 196 ng/u L. The gene *accA*, 1 of 4 subunits for the Acetyl-CoA Carboxylase enzyme, was suppressed by asRNA, producing a qPCR concentration of 63ng/u L. Antisense RNA for *accA* reduced the amount of Lux-S, a vital gene needed for propagating quorum-sensing signal molecules. Our purpose was to provide a more cumulative perspective for pathogenesis of disease within the microbiome.

15 **INTRODUCTION**

16 The Western diet includes high amounts of fats, sugars, and simple carbohydrates. Due to the Western diet,
17 diabetes, cancer, and many neurological disorders have proliferated and quickly increased the diagnosis
18 of these diseases (1). Ingestion of dietary fiber in the US and in European diets is approximated to be
19 more than a few grams per day. Non-digestible oligosaccharides give between 1 and 2 kcal/g of calories
20 (1). A cause for the prevalence of diseases may be the Western diet that lacks a high source of dietary
21 fiber. There are two main types of dietary fiber, soluble and insoluble fiber. Soluble fiber is found in fruits
22 and vegetables while insoluble fiber includes wheat, cellulose, and inulin. Insoluble fiber is necessary
23 because it maintains a healthy microbiome of the gut by allowing waste in the colon to become bulky
24 for the facile removal of fecal matter from the colon. Insoluble fiber allows for the absorption of water
25 to produce bowel movements more readily without blockage. Fiber regulates and promotes a healthy
26 gut microbiome. A healthy microbiome has many commensal and mutual symbiotic bacterial colonies.
27 A well-balanced microbiome prevents colon cancer by the apoptosis of cancerous cells (6). Butyrate,
28 a SCFA, suppresses tumors because it obstructs cell propagation and induces apoptosis when added to
29 different types of tumor cell lines (6). An important bacteria for maintaining homeostasis within the colon
30 and digestive tract, includes *E. coli*, a gram-negative bacteria that resides within the large intestines (6). *E.*
31 *coli* ferments glucose molecules into Butyrate. Butyrate is an attractive therapeutic molecule because
32 of its wide array of biological functions, such as its ability to serve as a histone deacetylase (HDAC)

33 inhibitor, an energy metabolite to produce ATP and a G protein-coupled receptor (GPCR) activator (2).
34 Intestinal bacteria use enzymes to split carbohydrates, with water, producing hydrogen, methane, carbon
35 dioxide, acetate, propionate, butyrate, and lactate. The end products from bacterial fermentation engender
36 energy for the colonic bacteria. A high fiber diet activates fermentation, which amplifies bacterial density
37 and fecal mass, increasing the viscosity of the stool. Approximately, about 30 g of bacteria is generated
38 for every 100 grams of carbohydrate made through fermentation (1). *E. coli* produces and secretes an
39 enzyme, acetyl-CoA carboxylase, breaking down glucose into butyrate, acetate, and propionate (6). Four
40 genes, *accA*, *accB-accC*, and *accD*, code for the translation of Acetyl-CoA carboxylase. These four
41 genes for Acetyl-CoA carboxylase can modify the composition of fatty acids and monitor the rate of
42 production. The four genes also monitor the over expression of ACCase with inserting one of the four
43 subunits to activate antisense RNA expression (19). Acetyl-CoA carboxylase hydrolyzes glucose into
44 short chain fatty acids including: propionate, acetate, and butyrate. SCFAs are hydrophilic, soluble, and
45 the bloodstream readily absorbs each SCFA. Many of the body's major organ systems as the nervous
46 system, skeletal-muscle system, and tissues catabolize acetate directly. Propionate decreases the liver's
47 production of cholesterol through the liver's ability to efficiently decay and clear Propionate, which blocks
48 its synthesis. The SCFAs initiate apoptosis(1). Fermentation of glucose to produce SCFAs also constrain
49 the development of disease-causing organisms by decreasing luminal and fecal pH (1). By lessening
50 the pH, the expression of unfavorable bacterial enzymes decreases due to reduced peptide degradation
51 and by the production of ammonia, amines, and phenolic compounds (1). In this study the gene, *accA*,
52 was analyzed through qPCR quantification. The concentration of *accA* was measured after culturing
53 *E. Coli* with high, medium, and low concentrations of glucose. The list of concentrations for glucose
54 administered include: 15mM, 7.5mM, 5mM, 200 u M, 50 u M, and 0u M. For example, ECV304 human
55 endothelial cells restricted the metabolism of glucose in response to high levels of glucose in the medium
56 by decreasing the rate of glucose phosphorylation (8). The regulation of metabolizing glucose suggests
57 that glucose phosphorylation is altered in vivo in response to high glucose levels (8). Also, the levels
58 of quorum sensing was analyzed. Quorum sensing is communication between bacterial cells through
59 a release of small signaling molecules called autoinducers. The autoinducers are released to regulate
60 the aggregation of cells and genetic expression. The autoinducers of gram negative bacteria consists
61 of homoserine lactones versus gram positive bacteria that are oligopeptides (35). We used qPCR to
62 quantify the amount of gene copies for the *accA* gene. Absolute qPCR produced a standard curve for
63 the genes from each bacterial grown in varied and set concentrations of glucose. Real-time PCR using
64 the LightCycler system (Roche Molecular Biochemicals, Mannheim, Germany) is accomplished by the
65 ceaseless quantification of the PCR products. The method is rapid and easy for the quantitative recognition
66 of microorganisms (17). The inhibition of genetic expression for *accA* will be inhibited through antisense
67 RNA. Antisense RNA innately occurs in bacterial cells as an immune response to foreign genetic material,
68 mainly foreign and viral DNA or RNA. The original protocell could constrain foreign and movable
69 DNA through transcription of antisense RNA, complementary to its specific DNA target sequence (18).
70 The asRNAs bind to the sequences flanking the ribosome-binding site and the start codon of the target
71 mRNAs (15). They block ribosomes from detecting the RBS, and therefore inhibit translation (15). In
72 the current study, antisense RNA was amplified through PCR of an antisense DNA sequence flanked
73 with *Xho*I and *Nco*I restriction sites, designing primer sequences of 30bps each. The PCR product
74 was ligated into the PHN1257 plasmid (Fig. 1). Competent bacterial cells were transformed with the
75 recombinant IPTG-PT-asRNA plasmid called PHN1257. The total RNA was extracted for qPCR analysis
76 to determine the number of gene copies for *accA*. Inhibiting genetic expression, at a intracellular level,
77 was quantified after bacterial cells for *E. Coli*, were transformed with recombinant DNA, the PHN1257
78 plasmid, containing the DNA insert. The asRNA blocked the mRNA expression of *accA*. Finding the
79 connection between the condition of the digestive system's microbiome, at a cellular and molecular level,
80 and disease can lead to devising alternative means of treatments. We want to find how gene regulation
81 with the different variations of growth factors as hormones, and the necessity for a high fiber diet may
82 treat disease from the gut to the whole human body. Therefore, regulating the environmental, genetic, and
83 the hormonal communication of signaling factors within the digestive tract can restore the homeostasis
84 from the intestinal microbiome to other organ systems.

85 **METHODS**

86 RNA Preparation *Escherichia coli* cells were grown on 25mL Luria Broth agar media plates. Transformed
87 bacterial competent cells, with (+antisense) and (-antisense) PTasRNA expression vectors, were grown
88 on LB agar plates with the kanamycin antibiotic and incubated at 37°C for 24hrs. Cells grown on agar
89 plates were inoculated into 4mL of LB liquid media with (+) and (-) PTasRNA bacterial cells expression
90 of asRNA for *accA* cultured with kanamycin. E.Z.N.A.® Bacterial RNA Kit allowed for rapid and
91 reliable isolation of high-quality total cellular RNA from a wide variety of bacterial species. Up to 3mL
92 of bacterial cell culture from the cells grown in the varied concentrations of glucose, the (+) asRNA, and
93 the (-)asRNA cells were centrifuged at 4,000 x g for 10 minutes at 4°C. The medium was discarded and
94 cells resuspended in 100µL Lysozyme/TE buffer. The solution was vortexed for 30 seconds. Incubation
95 occurred at 30°C for 10 minutes in a shaker-incubator. The lysis buffer of 350µL with 25mg of glass beads
96 were added. It was centrifuged for 5 minutes at maximum speed. RNA was extracted using HiBind®
97 RNA mini columns through RNA wash buffers, I and II. The RNA was eluted with 50µL of DEPC water.
98 Up to 1 x 10⁹ bacterial cells were processed. The system combined the reversible nucleic acid-binding
99 properties of Omega Bio-Tek's HiBind® matrix with the speed and versatility of spin column technology
100 to yield approximately 50-100 µg RNA. cDNA Preparation We used the OneScript Reverse Transcriptase
101 OneScript cDNA Synthesis kit by ABM. Approximately 1µg of RNA from each sample, High-glucose,
102 Medium-glucose, Low-glucose, and (-)glucose was added to 0.5µM oligonucleotides(dT) (10µM). For the
103 asRNA and (-) RNA, 1 µg of each total RNA extract was added to the initial primer/RNA and reaction
104 mixture. The Initial Primer/RNA mix: 1µg of total RNA, 1µL of oligo(dT), 1µL of dNTP (10mM) mix,
105 nuclease free-water for a 20µL reaction solution. The mixture was heated to 65°C for 5 minutes and
106 then incubated on ice for 1 minute. The reaction mixture of 4µL 5X RT buffer, 0.5µL of RNaseOFF,
107 and 1µL OneScript RTase was added to the initial primer/RNA mix in a 2µL microcentrifuge tube. The
108 cDNA was synthesized by incubating the tube for 50 minutes at 42°C. The reaction was stopped at
109 85°C for 5 minutes and chilled on ice. The cDNA was stored at -20°C. PCR A Promega PCR Master
110 Mix volume of 25µL was added to upstream and downstream primers each of 0.5µL specific for the
111 *accA* gene target. The concentrations of two cDNA samples added to the PCR master mix were 190ng
112 and 230ng plus nuclease free water. A 2X 1X upstream primer, 10µM 0.5–5.0µM 1 0.1–1.0µM, and a
113 downstream primer, 10µM 0.5–5.0µM 1 0.1–1.0µM, DNA template 1–5µL; 250ng Nuclease-Free Water
114 was mixed into a 50µL PCR reaction mixture. The thermocycler was set to a Denaturation of a 2-minute
115 initial denaturation step at 95 degrees Celsius. Other Subsequent denaturation steps were between 30
116 seconds and 1 minute. The Annealing step was optimized with annealing conditions by performing the
117 reaction starting approximately 5 degrees Celsius below the calculated melting temperature of the primers
118 and increasing the temperature in increments of 1 degree Celsius to the annealing temperature. The
119 annealing step was set at 30 seconds to 1 minute in 52 degrees Celsius. For the extension reaction with
120 Taq polymerase, we allowed 1 minute for DNA to be amplified at 72 degrees Celsius with a final extension
121 of 5 minutes at 72–74 degrees Celsius. The PCR thermocycler completed 40 cycles of amplification.
122 Plasmid Assembly The condition of the PCR products, without primer dimers and contamination, for the
123 target gene *accA*, were detected through agarose gel electrophoresis. The PCR products were confirmed
124 without primer dimers and contamination, the PCR products and the PTasRNA expression vector of the
125 plasmid PHN1257 were digested with the restriction enzymes XhoI (upstream) and NcoI (downstream)
126 (New England Biolabs XhoI- catalog R0146S- 1,000 units and NcoI- catalog R0193S- 1,000 units). Each
127 microcentrifuge tube was placed in the incubator for 30 minutes at 37°C. A heat block was heated to 90°C.
128 The PCR products of the *accA* gene were ligated into the PHN1257 plasmid by mixing 1µL of the DNA
129 insert with 2µL of the plasmids, adding 5µL of ligation mix, and then placing the tubes into a heat block
130 of 90°C for 15 minutes. (Takara Ligation Kit 6023). Competent bacterial cells were transformed with the
131 PHN1257 plasmid plus the antisense DNA insert of *accA*, for expressing (+)asRNA and (-)asRNA. The
132 competent cells were incubated with the recombinant DNA for 45 minutes at 37°C. Real time PCR The
133 cDNA from H-glucose, M-Glucose, L-glucose, and (-) was diluted into a 1:8 serial dilution. We pipetted
134 8µL of diluted cDNA into all wells of a clear 96 well plate. A 0.4µL of each primer pair mixture was
135 pipetted into a microcentrifuge tube with 10µL of SensiMix SYBR MasterMix, and with 1.2µL of DEPC
136 water. The SYBR reaction mixture of 12µL was then pipetted into the wells with the diluted and undiluted
137 cDNA. Optical film sealed the plate. To suspend all liquids to the bottom of the wells, we Centrifuged
138 the PCR plate for 2 minutes at 2500rpm. The RT-PCR Amplification Protocol (Roche Lightcycler 480
139 machine) began with a 3 min step at 95°C for 40 cycles with a step of 10 sec at 95°C, 45 sec at 65°C,

140 and 20 sec at 78°C with One step of 1 min at 95°C. One step of 1 min at 55°C 80 cycles of 10 sec each
141 starting at 55°C with a 0.5°C increment at each step up to 95°C. For the Roche Lightcycler 480 machine
142 the 96-well clear Roche plates were used for SYBR green detection.

143 RESULTS

144 The RNA Concentration and accA Genetic Expression of each Glucose Sample Escherichia coli MG1655
145 bacteria was grown in LB broth overnight at 37 o C with 15mM, 7.5mM, 5mM, and 0 mM of glucose
146 concentration for high-glucose, medium-glucose, low and zero glucose as a control, respectively (Fig. 2).
147 RNA was extracted from each sample and the concentrations determined by the Implen NanoPhotometer
148 250. The RNA concentrations for each sample measured were 1392ng/uL for high-glucose, 797 ng/uL for
149 medium-glucose, 608 ng/u L for low-glucose, and 179 ng/uL for the control. The high-glucose sample
150 had the highest amount of RNA compared to the medium to low and to the control. The RNA for each
151 sample was reverse transcribed into first strand cDNA and absolute quantification with qPCR was used to
152 measure the amount of the target gene, accA, produced by each sample. High-glucose had a Cp of 12.28
153 and the concentration of accA was 4.21E3 ng/u L. The Cp of sample medium-glucose equaled 16.51 with
154 a concentration of 3.75E2 and the low-glucose Cp was 14.08 with target gene concentration of 1.50E3
155 (Fig. 3). The control group had a Cp of 17.64 with a target gene concentration of 1.96E2. After loading a
156 96-well plate for qPCR with 5-fold dilution standards of each sample, the standards of each sample were
157 used to calculate a standard curve (Fig. 2) For the glucose concentrations of 200 uM, 50 uM, and 0uM
158 compared to their RNA concentrations, the standard deviation was 148 SD 204, 190 SD 252, and 107
159 SD 76, respectively. Comparing 200 uM to its control group, the difference between the samples was
160 statistically significant. The cells grown in 200uM had a more significant and larger production of accA,
161 with a p-value of 0.038, than cells grown in 0uM of glucose.

162 The qPCR results of asRNA for the target Gene accA Recombinant DNA was produced when the
163 PCR product of the gene insert, accA was ligated into the plasmid PHN1257 (Fig. 1), that was engineered
164 to amplify antisense RNA. The PCR product and the IPTG-PT-asRNAs plasmid of PHN1257 were cut
165 with the restriction enzymes XhoI and NcoI. The primers (Table. 1) each contained an extra 3 to 4 bps
166 of nucleic acids to accompany the sequences for XhoI and NcoI. The primers flanked the target DNA,
167 which totalled to 150 base pairs. The antisense sequence was constructed in a specific orientation where
168 the restriction enzymes, which NcoI normally flanks the forward primer, reversed positions. The XhoI
169 was repositioned to flank the forward primer, and the NcoI would flank the reverse primer, creating
170 the antisense sequence when inserted into the plasmid for PHN1257. The total RNA concentration for
171 the untransformed bacterial cells, or the positive control, equaled 739.44 ng/u L with an A260/A280
172 of 1.9. The positive control, No-asRNA, had a miRNA concentration of 334.98 ng/u L, including an
173 A260/A280 of 2 (Fig. 3). The RNA concentration for transformed bacterial cells with the asRNA of
174 accA PHN1257 plasmid was 279.28ng/u L, having an A260/A280 of 2.011. The miRNA concentration
175 of the cells with asRNA measured to 240.90 ng/u L and an A260/280 absorbency of 2.073 (Fig. 3).
176 The gene of accA was successfully suppressed by asRNA in vitro with 63 ng/u L measured for bacteria
177 cells transformed with the recombinant antisense PHN1257 plasmid DNA. The bacterial cells with the
178 PHN1257 plasmid but without the antisense gene target and insert produced 421.69 ng/uL for accA. There
179 was a 138asRNA for accA. A p-value of 0.027 showed highly significant data for the accA gene target
180 concentration of PHN1257(+)-asRNA versus PHN1257(-)-asRNA, or without asRNA. The gene of accA
181 was successfully suppressed by asRNA in vitro with 63 ng/uL measured for bacteria cells transformed
182 with the recombinant antisense PHN1257 plasmid DNA. The bacterial cells with the PHN1257 plasmid
183 but without the antisense gene target and insert produced 421.69 ng/uL for accA (Fig. 4). There was
184 a 138versus cells transcribing the asRNA for accA. A p-value of 0.027 showed highly significant data
185 for the accA gene target concentration of PHN1257(+)-asRNA versus PHN1257(-)-asRNA, or without
186 asRNA. Quantification of Lux-S Gene Expression Bacterial cells were transformed with the PHN1257
187 plasmid expressing asRNA to inhibit the genetic expression of the accA gene. RNA was extracted from
188 cells grown with 25u M glucose and 5u M of glucose. The cells grown with glucose in the medium
189 were also transformed with antisense expressing IPTG-PT-asRNA inducible PHN1257 plasmids. Cells
190 were cultured without (-)glucose but the expression of accA was also inhibited. A control, without
191 (-)glucose and (-)asRNA in vitro translation, was compared to each sample. The number of gene copies
192 for Lux-S was measured through qPCR and absolute quantification with a p-value;0.05,(Table. 2). The
193 (-)glucose-(+)-asRNA sample had a gene copy number of 199 and 2511 Lux-S copies for (-)glucose-(-)

194)asRNA. For the 25u M glucose-(+)asRNA and 5u M glucose-(+)asRNA produced 39,810 and 1×10^6
195 gene copies of Lux-S, respectively (Fig. 5). The samples with 5u M glucose-(+)asRNA exhibited the
196 highest amount of expression for Lux-S, which displays an increased amount of quorum sensing releasing
197 more autoinducer-2 molecules, directly affected by an increase sensitivity to glucose.

198 DISCUSSION

199 We assembled recombinant DNA plasmids from the IPTG-PT-asRNA of the PHN1257. The constructed
200 plasmid of PHN257 consisted of flanking inverted repeats that flank for the target DNA, rebuilding a paired
201 double-stranded RNA termini that inhibited the transcription of *accA* (15). The extracellular processes of
202 the microbiome were measured through increasing the gradient of glucose concentration. Transcription of
203 intracellular molecules were determined through qPCR. High levels of glucose increased the expression
204 of *accA*. Inhibition of *accA* was confirmed through qPCR results of 63 ng/u L for *accA*(+)asRNA versus
205 422 ng/u L for *accA*(-)asRNA. The amount of intercellular quorum sensing between bacterial cells was
206 quantified through qPCR. The volume of Lux-S was determined through qPCR. The qPCR results
207 demonstrated that the end yield of Lux-S and autoinducers, AI-2, cells are dependent on the supply of
208 glucose. The four genes *accA-accD* code for the subunits of the complex, Acetyl-CoA Carboxylase,
209 which catabolizes dietary fiber in the form of glucose to begin many biosynthetic processes. Acetyl-CoA
210 carboxylase (ACC) initiates the first step of fatty acid synthesis. During fatty acid synthesis, malonyl-
211 CoA is formed from acetyl-CoA, using energy from ATP and bicarbonate production (22). Glucose is
212 hydrolyzed into pyruvate, which is made into acetyl-CoA, forming acetate. Through the Wood-Ljungdahl
213 pathway, pyruvate loses two hydrogens, carbon dioxide loses an oxygen, altered into carbon monoxide,
214 and a methyl group is added to this reduction to make acetyl-CoA into Acetate (20). Butyrate is produced
215 when two molecules of acetyl-CoA combine into acetoacetyl-CoA. The acetoacetyl-CoA is transformed
216 into butyryl-CoA, or butyrate (20). Propionate is composed through the succinate or acrylate pathway
217 (41). PEP is broken into pyruvate which is further metabolized with water into succinate. The succinate is
218 reduced into propionyl-CoA, forming propionate. Through the acrylate pathway, lactate loses an oxygen,
219 forming propionate (20). Therefore, SCFAs are highly significant for initiating the downward cascades for
220 hormonal responses, regulating metabolism, controlling hunger signals to the brain, and affecting many
221 psychological behaviors. However, the rate of forming SCFAs is dependent on the glucose concentration
222 within the lumen of the intestines (16). Ferrais et al., measured the luminal glucose osmolarity and
223 concentrations of the small intestines. They found the assumptions of luminal glucose concentrations
224 being 50mM to 500mM to exhibit some errors (16). The previous studies measured glucose concentrations
225 but did not recognize how osmolality is affected by Na⁺ and K⁺ salts, amino acids, and peptides (16).
226 Ferrais et al., discovered the average of SI luminal osmolalities were approximately 100 mosmol/kg,
227 which were mainly hypertonic results. For an animal's diet, the SI glucose concentrations averaged
228 0.4-24 mM and ranged with time over a large amount of a SI region from 0.2 to 48 mM. E. Vinalis
229 et al found that high concentrations of glucose lessened the absorption of glucose in endothelial cells
230 called ECV304 cell lines. There was a 60The high glucose osmolities resulted in reduced V_{max} values
231 for 2-deoxyglucose uptake with a constant K_m, calculated from the Michaelis-Menten kinetic enzyme
232 equation (16). However, from our results, we found the genetic expression of *accA* to be proportional to
233 increasing glucose concentrations in E.Coli bacterial samples. After we cultured E. coli with different
234 levels of glucose, the RNA concentrations for each sample measured were 627 ng/u L for high-glucose,
235 452.88 ng/u L for medium-glucose, 361.72 ng/u L for low-glucose, and 137.60 ng/u L for the control. The
236 concentration of *accA*, in ng/u L, for each sample included: 4210, 375, 150, and 196 for H-glucose, M-
237 glucose, L-glucose, and No-Glucose respectively. We reached these specific results for genetic expression
238 amplified in conjunction with increased glucose concentration because the four subunits for the acetyl
239 carboxylase complex seem to be regulated only by the *accBC* lac operon and each gene, *accA* and *accD*,
240 are entirely independent of the *accBC* lac operon. When *accB* is overexpressed, *accBC* transcription is
241 blocked, but the overexpression of the other three gene products don't affect the *accBC* operon transcript
242 levels (22). When there is a high glucose concentration, the availability of *accB* increases, and the
243 transcription of the *accBC* lac operon is greatly reduced even after an exposure to a small amount of *accB*.
244 Although a high glucose concentration may have stymied the production of *accBC*, it did not seem to
245 inhibit the amplification of *accA*, our target gene and DNA sequence of study. E. Coli cells were grown
246 in 25u M and 5u M of glucose and transformed with antisense PHN1257 expressing IPTG-PT-asRNA
247 plasmids. Cell samples with 5u M glucose-(+)asRNA produced the highest amount of Lux-S gene (28).

248 Lux-S is needed to produce autoinducer two. Lux-s monitors the amount of biofilm, flagellum movement,
249 and monitors virulence. Biofilm increases the movement of bacteria into the bloodstream (35). The 5u
250 M glucose-(+)asRNA sample showed the most expression of Lux-S because Wang et al., (2005) found
251 adding 0.8g glucose to their bacterial culture and growth medium increased the activity at the promoter site
252 of the Lux-S gene. A glucose concentration of 5u M results in a normal exogenous osmolarity surrounding
253 bacterial cells within the microbiome of the lower digestive tract (28). Because cells were overly saturated
254 with a 25 u M concentration of glucose, we expected to find more release of autoinducer-2 signaling
255 molecules with more regulation of genetic expression. However, the over saturation of glucose at 25 u M
256 did not result in more genetic expression of Lux-S. Jesudhasan et al. (2010) proved that higher levels of
257 autoinducer-2 did not lead to increased genetic expression in Salmonella Typhimurium when cultured
258 in high concentrations of glucose (29). By transforming E.coli bacterial cells with IPTG-PT-asRNA
259 inducible vectors, the Lux-S gene was inhibited. When the Lux-S gene is mutated or suppressed, it
260 becomes more responsive to the concentration of glucose. Therefore, more transcription of Lux-S was
261 observed in cells cultured with 5u M glucose and less in activity from the 25u M sample. Because glucose
262 delays the movement of the Lux-S mutant strain, but does not inhibit bacterial growth, each (+)asRNA
263 sample appeared smaller and defected. Osaki et al., (2006) showed that Lux-S mutants can be smaller in
264 diameter with 8.0 mm versus 12.3 mm in its wild type (30). Figure. shows bacterial colonies expressing
265 antisense RNA with a smaller size versus cells without antisense RNA. Cell samples with (+)asRNA
266 transcription were smaller in size (30). Bacterial samples transformed with IPTG-PT-asRNA inducible
267 PHN1257 plasmids, designed to inhibit the accA gene, had the least measure of Lux-S expression. The
268 (-)glucose-(+)asRNA sample had the lowest amount of Lux-S expression of 199 gene copies. As a result,
269 when the Lux-S gene is mutated with less expression, the biofilm is thinner, looser, and displaying an
270 appearance of bacterial cells with defects. Lux-S forms a thicker and more viscous biofilm, which results
271 from a large amount of DNA released. The ample amounts of DNA released maintains a more solid
272 macromolecular matrix and consistency of the biofilm (39). Lux-S is required for AI-2 production and
273 for regulating gene expression in the early-log-growth phase. Pathogenic bacteria depend on biofilm
274 formation to attach to epithelial cells and tissues, spreading infectious diseases. Pathogenic bacteria
275 infects host cells by accumulating AI-2, exogenously, which then increases the amount and consistency of
276 the formation of biofilm (37). Streptococcus, a gram negative bacteria, results in the death of 2 million
277 people each year. Streptococcus lives symbiotically with other microflora in the nasopharynx region
278 of the respiratory system. After a month of commensal habitation, Streptococcus begins to infect other
279 parts of the body, leading to disease. To form biofilm for infection, the Lux-S gene must be activated. Its
280 excessive amplification and expression leads to a denser texture of biofilm (39). Lux-S monitors virulence
281 through regulation of the process of generating biofilm in the nasopharynx in mice with pneumonia.
282 Flagella expression increases with Lux-S mutation in the lungs and bloodstream. The Lux-S mutants
283 can infect the lungs or the bloodstream more rapidly than its wild-type strain (36). Flagellin increases
284 inflammation by activating TLR5 pathways, which translates pro-inflammatory genes within the MAPK
285 pathways. Flagella modulates virulence and pathogenesis by allowing a more rapid motility of bacteria,
286 infecting the colonization of host cells, and assisting infectious bacterial cells with entering the mucosal
287 layers (41). Pathogenic bacteria need to determine the autoinducer signals specific to their particular
288 species. Pathogenic bacteria require a specific order and assortment of virulent genes to infect, spreading
289 disease. For example, the different residues or R-groups of amino acids within autoinducers bind to
290 LUXR protein receptors in a conformation specific to the amino acid side chains within the binding
291 sites. The orientation of the AI to protein receptor binding produces varied types of side chain lengths
292 and amino acid substitutions (40). Microbiota in the gut respond to Lux-S transcription differently than
293 in the respiratory system. For example, pathogenic bacteria as E. coli EPEC has intraspecies signals
294 that help to colonize the small intestines. The small intestines is void of many commensal microflora.
295 The EHEC pathogenic form of E. coli conducts signals with other bacterial cell types and with host
296 cells. EHEC communicates through quorum sensing with other normal large intestine microflora. EHEC
297 infects through activating the genes called Locus of Enterocyte Effacement or LEE. The genes of LEE are
298 required for A/E lesions to form when EHEC cells attach to and efface from epithelial cells, amplifying the
299 level of pathogenicity (34). Autoinducer 2 requires the genetic expression and translation of Lux-S. When
300 Lux-S and autoinducer-2 is less regulated and overexpressed, infectious bacteria can propagate in stressful
301 environments with high acidity and salinity (32). Kendall et al., (2008) demonstrated S.pyogenes adapting
302 to acidic conditions when the luxS/AI-2 system was unregulated. Autoinducer 3 is not dependent on

303 expression of the Lux-S gene. Lux-S genetic mutants impedes the production of AI-3 (31-32). As a result,
304 the pathogenic E.coli, EHEC, collects signals from host cells in the form of hormones as epinephrine.
305 AI-3 has the ability to communicate with the transmembrane protein called Qsec (31). Bone marrow
306 white blood cells, as macrophages, can be incubated with synthetic 3-oxo-C12-HSL and C4-HSL, for
307 24 hours. The induced apoptotic activity of 3-oxo-C12-HSL can be demonstrated in neutrophils and
308 monocytic cell lines U-937 and P388D1, respectively (7). Cells treated with 3-oxo-C12-HSL can reveal
309 morphological alterations indicative of apoptosis (3). Qualitative data of apoptosis can be assayed with
310 BIORAD with live cell fluorescence microscopy. Bone marrow cells can be cultured with an assay called
311 the pSIVA REAL-TIME Apoptosis Fluorescent Microscopy Kit. The assay of apoptosis can give us real
312 time data-analysis of apoptotic signaling at the cell surface (17).

313 CONCLUSION

314 We attempted to learn more about the fluctuations within the exogenous composition of the extracellular
315 matrix and from the effects of genetic mutations on the intracellular downward biochemical cascades.
316 We intended to show an intense and acute budding of pathogenesis when the intracellular processing
317 of intercellular signaling molecules are combined with genetic and external changes that innumerable
318 alter the intestinal microflora. The results observed displayed the RNA concentration for bacterial cells,
319 expressing asRNA of *accA*, included a concentration of 279.28 ng/u L, having an A260/A280 of 2.011. The
320 miRNA concentration of the cells with asRNA measured to 240.90 ng/u L and an A260/280 absorbency of
321 2.073, with a p-value ≤ 0.05 . The concentration for cells without antisense RNA was 422 ng/u L compared
322 to 63ng/u L for cells expressing asRNA. Antisense RNA transcription also occurs in bacteria naturally.
323 Naturally occurring asRNAs were first observed in bacteria more than 30 years ago and were approximated
324 even earlier for the bacteriophage of lambda (22). In archaea, the first case of the antisense control of gene
325 expression was reported in 1993 for the extremely halophilic prokaryotic cells called the *Halobacterium*
326 *salinarum*, with an asRNA complementary to the first 151 nucleotides (nt) of the transcript T1 (22). From
327 dietary fiber, or undigested carbohydrates, SCFAS are produced and can catalyze hormonal signals within
328 enteroendocrine cells. SCFAS can bind to G-protein coupled receptors, leading to a downward cascade of
329 reactions within endocrine cells. For example, SCFAs bind the G-protein coupled receptor 41, which then
330 causes the secretion of the hormone PYY. Peptide YY increases the rate of digestion and conserves the
331 energy from the diet (21). Including more dietary fiber in the Western Style diet is one of the best ways
332 to restore balance and a healthy condition of the intestinal microbiome. However, there may be more
333 alternatives for treating dysbiosis within the microbiome of the gut. Since 70improve insulin sensitivity,
334 fight obesity, eradicate colon cancer cells, and reduce mental disorders as depression, the human gut
335 microbiota may be a source of a conduit for treating many human diseases. For example, there has
336 been found a tumor-inhibiting molecule released by a probiotic strain of bacteria. The *L. casei* strain of
337 ATCC 334 produces ferrichrome, which delays the metastasis of colon cancer by activating the c-Jun
338 N-terminal kinase pathway of apoptosis (27). Increasing production of ClpB, a chaperone protein secreted
339 by *E.coli*, reduced food intake, limit meal patterns, and stimulated intestinal hormones in mice as a
340 glucagon-like peptide 1, an antihyperglycemic protein (27). Another study found therapeutic opportunities
341 for inflammatory diseases through isolating 17 clostridium strains and re-engineering mixtures of those
342 strains, which decreased colitis and increased Treg cells in rodents. Inflammation of the airways due
343 to allergies and inflammatory colitis have been shown to be remedied by interleukin-10, a cytokine
344 expressed by the bacteria, *Lactococcus lactis* (27). Isolating microbial organisms with the possibility
345 of providing alternative therapies for disease is extremely favorable for future research. Synbiotics is
346 a territory minutely explored, but is gaining noticeability. For future studies, we are greatly interested
347 in the live cell imaging of bone marrow cells lines cultured with 3-oxo-C12-HSL, displaying real time
348 apoptotic activity at the cell membrane level. The 3-oxo-C12-HSL is a *P. aeruginosa* signal molecule
349 homoserine lactone reported to inhibit function of PPARs in mammalian cells, combating lung disease
350 (24). Bacterial cells cultured in high-glucose to a zero glucose concentration showed a decreasing range
351 of genetic expression for our target gene, *accA*. Like we hypothesized an increased amount of available
352 glucose showed the highest measure of transcription of *accA*. We silenced the *accA* gene with antisense
353 RNA, using a, IPTG-inducible vector called PHN1257. There was a 138antisense PHN1257 versus cells
354 with no antisense RNA in vitro transcription. We wanted to model how high levels of glucose, from
355 high fiber intake, increases production of *accA* into mRNA for translation into acetyl-CoA carboxylase
356 enzyme, which produce SCFAs. We also attempted to show how a gene knockout of *accA* with asRNA

357 can decrease genetic expression. In many diseases of the colon, an excess of glucose or hyperglycemia can
358 lead to inhibition of genetic expression of pertinent genes needed for metabolism and fatty acid synthesis.
359 We found that SCFAs, metabolites from the fermentation of insoluble fiber and glucose by E.Coli bacteria,
360 has many beneficial properties and characteristics. Butyrate can bind transmembrane proteins, leading
361 to a cascade of cellular reactions as apoptosis through quorum sensing. The intracellular signals induce
362 communication between bacterial cells to endothelial cells of the large intestines. Therefore, with the
363 inhibition of the gene *accA*, the fermentation of glucose can be delayed leading to decreased formation of
364 the catabolite of butyrate and silencing the quorum sensing between cells. The microbiome of bacterial
365 cells can communicate with the gut, using a variety of chemical idioms, which, their host cells can
366 detect (25). This review has considered the relevance for the link between an individual's overall health
367 to bacterial cells' sensitivity to glucose, and the availability of metabolites. However, we focused on
368 presenting evidence for the impact of effects from bacterial cells potential for detecting host signalling
369 molecules upon (9). A group of chemical molecules for bacterial language expression and transfer
370 includes homoserine lactones, which are the most heavily studied. When infection occurs, homoserine
371 lactones are formed, and interrelate with the immune system (26). Hormones affect the balance of flora
372 within the microbiome. According to Hur Vi. Linn et al (2015), SCFAs are also subunits of signaling
373 molecules. The G protein-coupled receptors called Free fatty acid receptor 2 (FFAR2, GPR43) and FFAR3
374 (GPR41) have been identified as receptors for SCFAs. Acetate stimulates FFAR2 in vitro; propionate
375 presents similar traits of binding to a receptor and triggering downward cascade responses on FFAR2 and
376 FFAR3; and butyrate only activates FFAR3 (26). When bacterial genetic expression of the genes *accA*,
377 *accBC*, and *accD* are inhibited, the production of SCFAs is disrupted, delaying hormonal responses. The
378 fermentation of glucose by E.Coli leads to SCFAs binding to G-coupled protein receptors that increase
379 or decrease cell-to-cell signaling (12). The SCFA receptors FFAR2 and FFAR3 are both expressed in
380 the intestine and maintain symbiosis with adjacent enteroendocrine cells in the mucosal lining of the
381 digestive tract that express the Peptide YY (PYY). FFAR3 deficiency in mice was associated with a
382 reduced involvement of bacteria from the microflora, which allowed an increased expression of PYY in
383 the plasma (12). The purpose for our study was to construct a cumulative understanding of the processes
384 within the inner mechanisms of the intestinal microbiome. The microbiome is a vast organ, so our aim
385 was to attempt to compile a small part of its large navigational map to identify possible locales for future
386 synbiotic research and study.

387 ACKNOWLEDGEMENTS

388 Special thanks are given to Dr. Cory Tobin and Melissa Draeger from TheLAB in Los Angeles, CA. They
389 were responsible for ordering and delivering all materials I bought for this project. Much thanks is given
390 for their commitment to assisting me with tips and solutions for laboratory procedures. Thank you to Dr.
391 Tobin for helping me frame the structure of this project. He was always available for answering questions
392 and giving much guidance. Thank You!

393 References

394 S. Joanne, "Fiber and Prebiotics: Mechanisms and Health Benefits." *Nutrients* 5.4 (2013): 1417–1435.
395 PMC. Web. 5 July 2018. M.W. Bourassaab, S.J. IshraqAlimab, Bultmanc, R.R. Rajiv "Butyrate, '
396 neuroepigenetics and the gut microbiome: Can a high fiber diet improve brain health?'" *Neuroscience*
397 *Letters* 625 (2016): 56-63. Document . M., Vital, C. R., Penton, Q., Wang, V. B., Young, D. A.,
398 Antonopoulos, M. L., Sogin, et al. (2013). A gene-targeted approach to investigate the intestinal butyrate-
399 producing bacterial community. *Microbiome* 1, 8. doi: 10.1186/2049-2618-1-8 T.K. Goulas, A.K. Goulas,
400 G. Tzortzis, G.R. Gibson, 2007b. Molecular cloning and comparative analysis of four beta-galactosidase
401 genes from *Bifidobacterium bifidum* NCIMB41171. *Appl Microbiol Biotechnol* 76:1365–72. N. Yin,
402 T.M.A. Santos, G.K. Auer, J.A. Crooks, P.M. Oliver, D.B. Weibel, *Bacterial Cellulose as a Substrate for*
403 *Microbial Cell Culture*. Liu S-J, ed. *Applied and Environmental Microbiology*. 2014;80(6):1926-1932.
404 doi:10.1128/AEM.03452-13. D.R. Donohoe, et al. A gnotobiotic mouse model demonstrates that dietary
405 fiber protects against colorectal tumorigenesis in a microbiota- and butyrate-dependent manner. *Cancer*
406 *Discov*. 2014; 4:1387–1397. A. Barcenilla, et al. Phylogenetic relationships of butyrate-producing
407 bacteria from the human gut. *Appl. Environ. Microbiol.* 66, 1654–1661 (2000). Francesc Vinals, Achim
408 Gross, Xavier Testar, Manuel Palacin, Peter Rösen, Antonio Zorzano, High glucose concentrations inhibit
409 glucose phosphorylation, but not glucose transport, in human endothelial cells, *Biochimica et Biophysica*
410 *Acta (BBA) - Molecular Cell Research*, Volume 1450, Issue 2, 1999, Pages 119-129, ISSN 0167-4889

411 S. Sandrini, M. Aldriwesh, M. Aldriwesh, P. Freestone, (2015) Microbial endocrinology: host-bacteria
412 communication within the gut microbiome. *J Endocrinol* 225(2):R21–R34. S.T. Freestone, B.L. Bassler,
413 Bacterial Quorum Sensing: Its Role in Virulence and Possibilities for Its Control. Cold Spring Harbor
414 Perspectives in Medicine. 2012;2(11):a012427. doi:10.1101/cshperspect.a012427. K. Tateda, et al.
415 The *Pseudomonas aeruginosa* autoinducer N-3-oxododecanoyl homoserine lactone accelerates apoptosis
416 in macrophages and neutrophils. *Infect. Immun.* 71, 5785–5793 (2003). J.M. Ridlon, D.J. Kang,
417 P.B. Hylemon, J.S. Bajaj, Bile Acids and the Gut Microbiome. Current opinion in gastroenterology.
418 2014;30(3):332-338.doi:10.1097/MOG.000000000000057. H.V. Lin, A. Frassetto, E.J. Kowalik Jr, et al.
419 Butyrate and propionate protect against diet-induced obesity and regulate gut hormones via free fatty
420 acid receptor 3-independent mechanisms. *PLoS One* 2012;7:e35240. 10.1371/journal.pone.0035240
421 K. Pokusaeva, G.F. Fitzgerald, D. Sinderen, Carbohydrate metabolism in Bifidobacteria. *Genes Nutr.*
422 2011;6:285–306. N. Nakashima, T. Tamura, (2009) Conditional gene silencing of multiple genes with
423 anti-sense RNAs and generation of a mutator strain of *Escherichia coli*. *Nucleic Acids Res* 37:e103 R.P.
424 Ferraris, S. Yasharpour, K.C.K. Lloid, R.Mirzayan, J.M. Diamond, (1990) Luminal glucose concentration
425 in the gut under normal conditions. *Am. J. Physiol.*, 259, G820–G837. 17. H. Maeda, C. Fujimoto,
426 Y. Haruki, T. Maeda, S. Koikeguchi, M. Petelin, H. Arai, I. Tanimoto, F. Nishimura, S. Takashiba,
427 Quantitative real-time PCR using TaqMan and SYBR Green for *Actinobacillus actinomycetemcomitans*,
428 *Porphyromonas gingivalis*, *Prevotella intermedia*, *tetQ* gene and total bacteria, *FEMS Immunology and*
429 *Medical Microbiology*, Volume 39, Issue 1, 1 October 2003, Pages 81– 86, [https://doi.org/10.1016/S0928-](https://doi.org/10.1016/S0928-8244(03)00224-4)
430 [8244\(03\)00224-4](https://doi.org/10.1016/S0928-8244(03)00224-4) 18. B.R. tenOever, The Evolution of Antiviral Defense Systems. *Cell Host Microbe*.
431 2016;19:142–149. doi: 10.1016/j.chom.2016.01.006. 19. K. Ali, and T. Aruna, "Recent advances in acetyl
432 CoA carboxylase: a key enzyme of fatty acid biosynthesis in plants." *Intl JAppl Biol Pharmac Technol*
433 7 (2016): 264-277. 20. A. Koh, et al. "From dietary fiber to host physiology: short-chain fatty acids
434 as key bacterial metabolites." *Cell* 165.6 (2016): 1332-1345. 21. K.Y. Hur, M.S. Lee, "Gut microbiota
435 and metabolic disorders." *Diabetes and metabolism journal* 39.3 (2015): 198-203. 22. E.S. James, J.E.
436 Cronan, "Expression of two *Escherichia coli* acetyl-CoA carboxylase subunits is autoregulated." *Journal of*
437 *Biological Chemistry* 279.4 (2004): 2520-2527. 23. J. Georg, R.H. Wolfgang, "cis-antisense RNA, another
438 level of gene regulation in bacteria." *Microbiology and Molecular Biology Reviews* 75.2 (2011): 286-300.
439 24. M.A. Cooley, C. Whittall, M.S. Rolph, "Pseudomonas signal molecule 3-oxo-C12-homoserine
440 lactone interferes with binding of rosiglitazone to human PPAR γ ." *Microbes and infection* 12.3 (2010):
441 231-237. 25. C.M. Waters, B.L. Bassler, "Quorum sensing: cell-to-cell communication in bacteria." *Annu. Rev. Cell Dev. Biol.* 21 (2005): 319-346. 26. G. Telford, et al. "The *Pseudomonas aeruginosa*
443 Quorum-Sensing Signal Molecule N-(3-Oxododecanoyl)-L-Homoserine Lactone Has Immunomodulatory
444 Activity." *Infection and immunity* 66.1 (1998): 36-42. 27. S.V. Lynch, O. Pedersen, "The human intestinal
445 microbiome in health and disease." *New England Journal of Medicine* 375.24 (2016): 2369-2379. 28. L.
446 Wang, et al. "Cyclic AMP (cAMP) and cAMP receptor protein influence both synthesis and uptake of
447 extracellular autoinducer 2 in *Escherichia coli*." *Journal of bacteriology* 187.6 (2005): 2066-2076. 29.
448 P.R. Jesudhasan, et al. "Transcriptome analysis of genes controlled by *luxS*/autoinducer-2 in *Salmonella*
449 *enterica* serovar Typhimurium." *Foodborne pathogens and disease* 7.4 (2010): 399-410. 30. T. Osaki, et al.
450 "Mutation of *luxS* affects motility and infectivity of *Helicobacter pylori* in gastric mucosa of a Mongolian
451 gerbil model." *Journal of medical microbiology* 55.11 (2006): 1477-1485. 31. M.M. Kendall, D.A. Rasko,
452 V. Sperandio, "Global effects of the cell-to-cell signaling molecules autoinducer-2, autoinducer-3, and
453 epinephrine in a *luxS* mutant of enterohemorrhagic *Escherichia coli*." *Infection and immunity* 75.10
454 (2007): 4875-4884. 32. M. Kendall, et al., "Functional analysis of the group A streptococcal *luxS*/AI-2
455 system in metabolism, adaptation to stress and interaction with host cells." *BMC microbiology* 8.1 (2008):
456 188. 33. M. Labandeira-Rey, et al., "Inactivation of the *Haemophilus ducreyi luxS* gene affects the
457 virulence of this pathogen in human subjects." *Journal of Infectious Diseases* 200.3 (2009): 409-416.
458 34. A. Vendeville, et al., "Making 'sense' of metabolism: autoinducer-2, *LuxS* and pathogenic bacteria." *Nature Reviews Microbiology* 3.5 (2005): 383. 35. L. Xu, et al., "Role of the *luxS* quorum-sensing
459 system in biofilm formation and virulence of *Staphylococcus epidermidis*." *Infection and immunity* 74.1
460 (2006): 488-496. 36. J.E. Vidal, et al., "The *LuxS*-dependent quorum sensing system regulates early
462 biofilm formation by *Streptococcus pneumoniae* strain D39." *Infection and immunity* (2011): IAI-05186.
463 37. J.E. Vidal, et al., "Quorum sensing systems *LuxS*/AI-2 and Com regulate *Streptococcus pneumoniae*
464 biofilms in a bioreactor with living cultures of human respiratory cells." *Infection and immunity* (2013):
465 IAI-01096. 38. Y. Yang, et al., "Quorum-sensing gene *luxS* regulates flagella expression and Shiga-like

466 toxin production in F18ab Escherichia coli." Canadian journal of microbiology 60.6 (2014): 355-361.
467 39. C. Trappetti, et al., "LuxS mediates iron-dependent biofilm formation, competence and fratricide
468 in Streptococcus pneumoniae." Infection and immunity (2011): IAI-05644. 40. A. Jayaraman, K.W.
469 Thomas, "Bacterial quorum sensing: signals, circuits, and implications for biofilms and disease." Annu.
470 Rev. Biomed. Eng. 10 (2008): 145-167. 41. U. Emilio, (2015). Shifts in metabolic hydrogen sinks in the
471 methanogenesis-inhibited ruminal fermentation: a meta-analysis. Frontiers in Microbiology, 6, 37.

Table 1 (on next page)

Primers for amplifying the Lux-S gene, antisense RNA for accA, and the accA gene.

Table 1. Primers for PCR Amplification and qPCR Analysis. To produce antisense RNA for *accA* inhibition the restriction enzyme site for *XhoI* was sequenced with the forward primer for *accA*. The restriction enzyme *NcoI* was added to the reverse primer for *accA*. Through PCR amplification, the per products were composed of antisense DNA for the *accA* gene. The PCR product would be inverted when inserted into the IPTG-PT-asRNA inducible PHN1257 plasmid, forming recombinant DNA plasmids for asRNA transcription in vitro. The plasmids with recombinant antisense DNA were transformed into bacterial competent cells for qPCR analysis of the *accA* gene. The primers for the *Lux-S* gene were applied to quantify the number of gene copies from qPCR analysis for cells grown in glucose enhanced samples. The primers for the *accA* gene were used for the quantification of the *accA* gene from the samples cultured with an increasing gradient of glucose solutions.

Primers	DNA Sequence
<i>XhoI</i> + <i>accA</i> Forward	GAGATGAGTCTGAATTTTCCTTGATT
<i>NcoI</i> + <i>accA</i> Reverse	TGGCAGTTCATCGCTTTTTTTCAC
<i>Lux-S</i> Forward	CATACCCTGGAACATCTGTTTGC
<i>Lux-S</i> Reverse	AGTTCCTGCACTTTCAGCACATC
<i>accA</i> Forward	TCATCACCTTTATCGACACCCC
<i>accA</i> Reverse	TTCACCTTATCGCCCACGCC

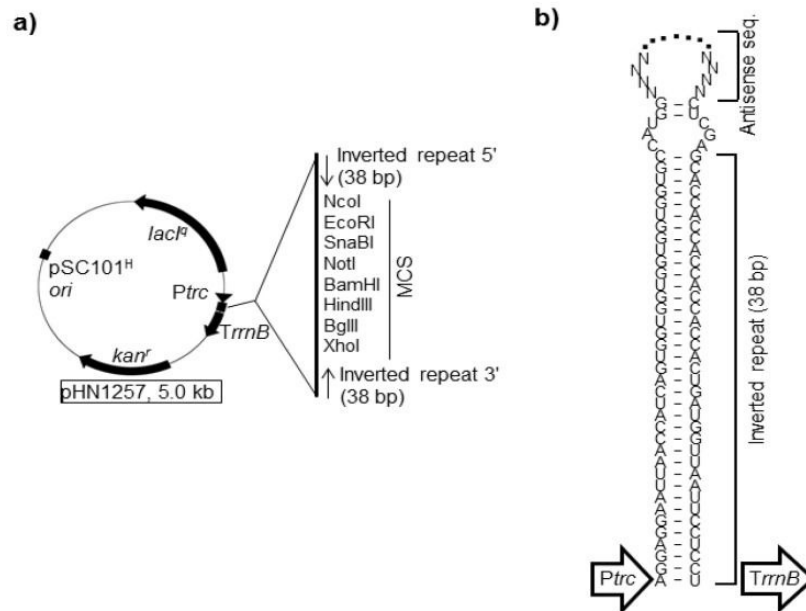
Figure 1(on next page)

Displays an image of the antisense RNA Vector, PHN1257.

Fig. 1 Plasmid Assembly and Gene Silencing the PCR products and the PTasRNA expression vector of the plasmid PHN1257 were digested with the restriction enzymes XhoI (upstream) and NcoI (downstream). After the restriction digestion, the antisense PCR product was ligated into the IPTG-PTasRNA inducible vector of PHN1257 at the multiple cloning site.

doi: [10.3390/ijms15022773](https://doi.org/10.3390/ijms15022773)

This article is an open access article distributed under the terms and conditions of the Creative Commons Attribution license (<http://creativecommons.org/licenses/by/3.0/>).



<https://www.ncbi.nlm.nih.gov/pmc/articles/PMC3958881/figure/f6-ijms-15-02773/>

Figure 2 (on next page)

Displays results for glucose affecting dsDNA and RNA concentration.

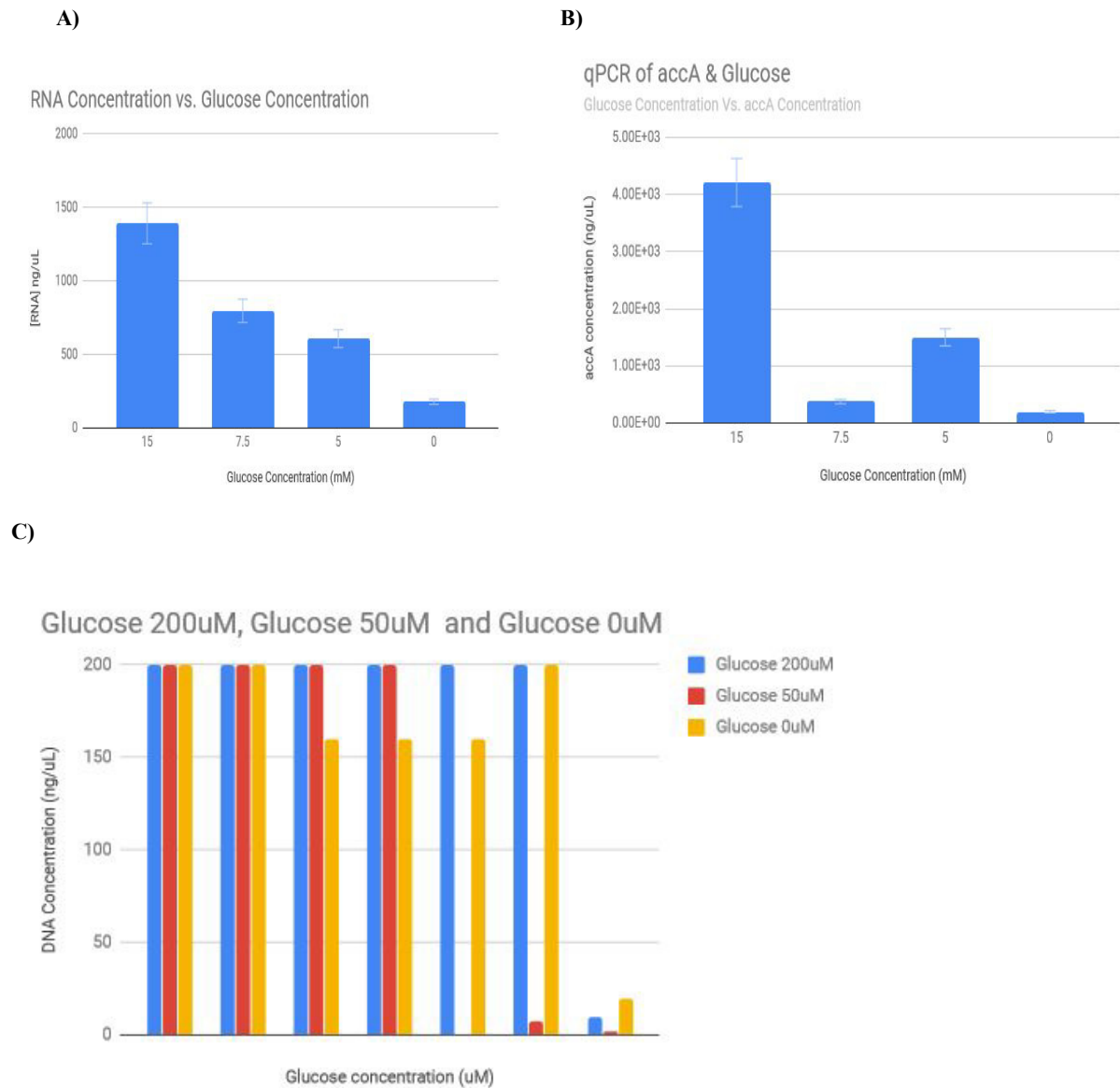
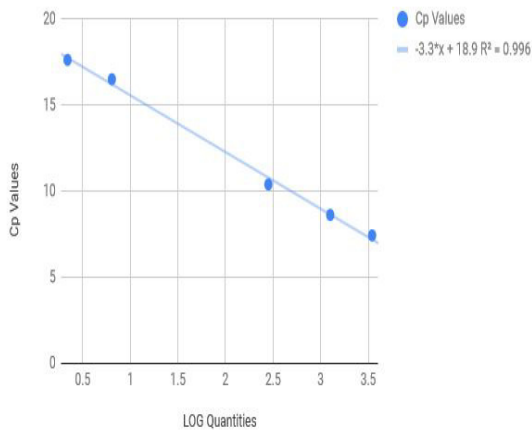


Fig. 2 A) Glucose concentrations of 15mM, 7.5mM, 5mM, and the control samples each had RNA concentrations, in ng/uL, 1392, 797, 608, 179, respectively. The bacterial sample with 15mM glucose, a high concentration, had the largest measure of RNA, noting a direct proportional link between glucose and genetic expression in gram negative bacteria as E.coli. **B)** Includes qPCR results for 15mM, 7.5mM, 5mM, and 0mM. The samples with 15mM and 5mM glucose displayed the most genetic activity of accA transcription, measuring accA concentrations at 4,210 ng/uL and 1,500ng/uL respectively. The accA qPCR concentrations for 7.5mM equaled 372 ng/uL and 196 ng/uL for 0mM. **C)** Displays OD260 results for samples of E.coli grown in medium enhanced with 200uM, 50uM, 0mM of glucose.

Figure 3 (on next page)

The qPCR results for quantifying accA concentration and the gene copy number.

Standard Curve of Glucose Sample Concentrations



Standard Curve for (+) asRNA and (-) asRNA of accA

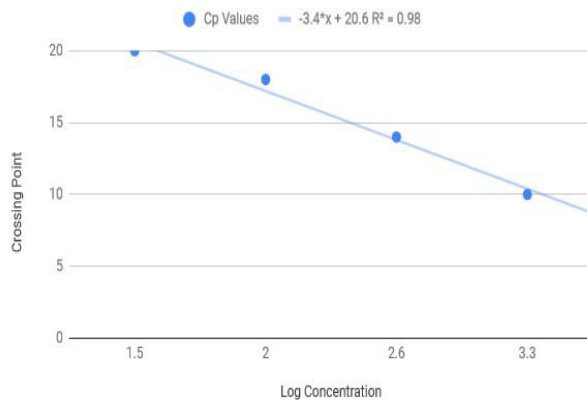


Fig. 3 Standard Curves for Quantifying Gene Copies The RNA for each sample was reverse transcribed into first strand cDNA and absolute quantification with qPCR was used to measure the amount of the target gene, *accA*, produced by each sample. High-glucose had a Cp of 12.28 and the concentration of *accA* was 4.21E3 ng/uL. The Cp of sample medium-glucose equaled 16.51 with a concentration of 3.75E2 and the low-glucose Cp was 14.08 with target gene concentration of 1.50E3. The gene of *accA* was successfully suppressed by asRNA in vitro with 63 ng/uL measured for bacteria cells transformed with the recombinant antisense PHN1257 plasmid DNA. The bacterial cells with the PHN1257 plasmid but without the antisense gene target and insert produced 421.69 ng/uL for *accA*. There was a 138% percent difference between cells not expressing asRNA versus cells transcribing the asRNA for *accA*. A p-value of 0.027 showed highly significant data for the *accA* gene target concentration of PHN1257(+)*asRNA* versus PHN1257(-)*asRNA*, or without asRNA.

Figure 4(on next page)

Gene Copies for Lux-S determined through qPCR measurement .

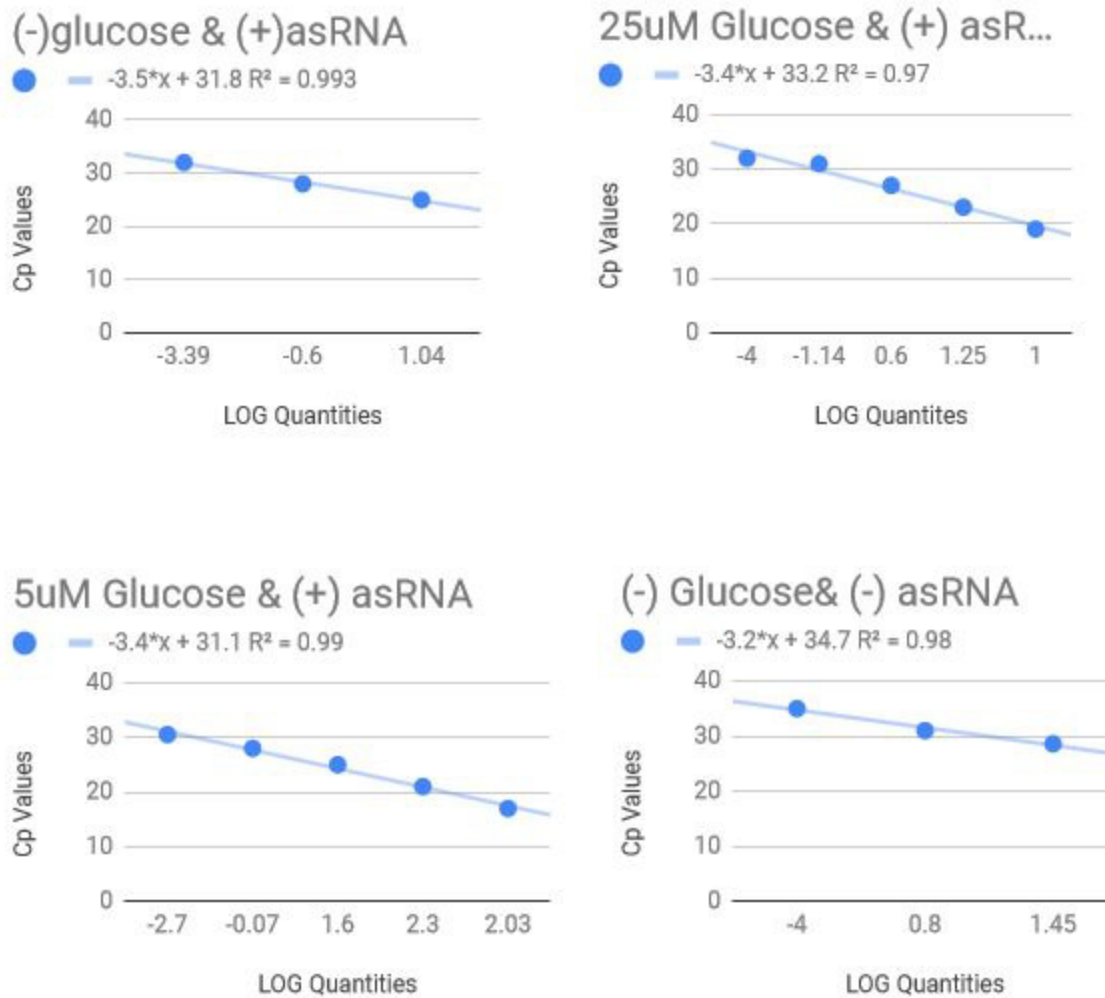


Fig. 4 qPCR Results for Lux-S The number of gene copies for Lux-S was measured through qPCR and absolute quantification. The (-)glucose-(+)asRNA sample had a gene copy number of 199 and 2511 Lux-S copies for (-)glucose(-)asRNA. For the 25uM glucose-(+)asRNA and 5uM glucose-(+)asRNA produced 39,810 and 1×10^6 gene copies of Lux-S, respectively.

Table 2 (on next page)

Anova Results of each experimental sample for quantifying qPCR gene copies.

ANOVA Results of qPCR Gene Copies

	Lux-S-glu/(+) asRNA	Lux-S-glu/(+) asRNA	(-)glu(-)asRNA	accA (+)glu/accA (-) glu	accA (+)glu/accA (-) glu
1	2511	316228	1000000	186	100
2	2000	26915.4	1000000	79	32
3	745	17783	39810	18	5
4	199	251	151286	7.4	3
n	4	4	4	4	4
X	1363.750	90294.350	547774.000	72.600	35.000
s	1074.010	151028.260	524165.009	81.920	45.306
X_{ave}	127907.940				

total	19	1798315304447.048
-------	----	-------------------

source	df	SS	MS	F	P-value
treatments	4	905636341810.108	226409085452.527	3.8044	0.0250
error	15	892678962636.940	59511930842.463		
total	19	1798315304447.048			

Figure 5 (on next page)

Graph of each sample with LuxS, expressing asRNA, enhanced with glucose, without glucose, and without asRNA.

